J Ind Microbiol Biotechnol (2015) 42:1449–1461
DOI 10.1007/s10295-015-1653-2

BIOCATALYSIS

Structural and functional analysis of a low-temperature-active alkaline esterase from South China Sea marine sediment microbial metagenomic library

Yongfei Hu[1,2,3] · Yinghui Liu[4] · Jing Li[1,2] · Yanbin Feng[4] · Na Lu[1,2] · Baoli Zhu[1,2,3] · Song Xue[4]

Received: 24 March 2015 / Accepted: 30 June 2015 / Published online: 8 September 2015

Abstract A low-temperature-active alkaline esterase, Est12, from a marine sediment metagenomic fosmid library was identified. Est12 prefers short- and middle-chain *p*-nitrophenol esters as substrate with optimum temperature and pH value of 50 °C and 9.0, respectively, and nearly 50 % of maximum activity retained at 5 °C. The hydrolysis activity of Est12 was stable at 40 °C. Ca^{2+} especially activated the activity of Est12 to about 151 % of the control. DEPC and PMSF inhibited the activity of Est12 to 34 and 25 %, respectively. In addition, Est12 was more tolerable to methanol compared to other organic solvents tested. The crystal structure of Est12 at 1.39 Å resolution showed that the cap domain which is composed of an α-helix and a flexible region resulted in a relatively wide spectrum of substrate, with *p*-nitrophenol caproate as the preferred one. Furthermore, the flexible cap domain and the high percentage of Gly, Ser, and Met may play important roles in the adaptation of Est12 to low temperature.

Keywords Marine sediment · Fosmid library · Esterase · Low-temperature active · Crystal structure

Introduction

Lipolytic enzymes such as esterases (EC 3.1.1.1) and lipases (EC 3.1.1.3) represent a group of hydrolases catalyzing both the hydrolysis and synthesis of ester bonds and are widely distributed in animals, plants, and microorganisms. The lipolytic enzymes belong to serine hydrolysis superfamily. Therefore, the activities of these enzymes rely mainly on a catalytic triad usually formed by Ser, His, and Asp residues. The enzymes with valued features, such as broad substrate specificity, stability in organic solvents, and stereoselectivity, become one of the most important groups of biocatalysts for biotechnological applications [3, 28]. Most of the lipolytic enzymes used in industry are microbial enzymes, which have been classified into eight families by Arpigny and Jaeger [3]. Recently identified lipases and esterases such as LipG [35], EstA [6], and LipEH166 [32] further enriched the families of lipolytic enzymes. Identification of novel esterases and lipases will increase the diversity of lipolytic enzymes and help in selection of suitable biocatalyst for challenging reactions [47].

Many attempts in the past have been made to find new lipolytic enzymes from culturable microorganisms of various environments. However, the culturable microbes account for only a tiny fraction of the microbial community, therefore, limiting the spectrum of searching for

Y. Hu and Y. Liu are contributed equally to this work.

Electronic supplementary material The online version of this article (doi:10.1007/s10295-015-1653-2) contains supplementary material, which is available to authorized users.

✉ Baoli Zhu
zhubaoli@im.ac.cn

✉ Song Xue
xuesong@dicp.ac.cn

1 CAS Key Laboratory of Pathogenic Microbiology and Immunology, Institute of Microbiology, Chinese Academy of Sciences, Beijing 100101, China

2 Beijing Key Laboratory of Microbial Drug Resistance and Resistome, Beijing 100101, China

3 Collaborative Innovation Center for Diagnosis and Treatment of Infectious Diseases, The First Affiliated Hospital, College of Medicine, Zhejiang University, Hangzhou 310006, China

4 Marine Bioengineering Group, Dalian Institute of Chemical Physics, Chinese Academy of Sciences, Dalian 116023, China

new enzymes. By contrast, more than 99 % of uncultured microorganisms in most environments represent a large gene pool for biotechnological exploitation [2, 16]. Metagenomics, a cultivation-independent method to study microbial communities is one of the key technologies used to access and investigate the uncultured microorganisms [41]. This strategy has been successfully applied to isolate novel biocatalysts such as chitinases [7], amylases [58], protease [20], 4-hydroxybutyrate dehydrogenases [23], lipases and esterases [24, 36], nitrilases [11], and cellulase [56].

Marine environments including the deep-sea sediment are considered to be the largest ecosystems on the earth [39]. Microorganisms inhabiting in such environment are exposed to extremes in pressure, salinity, temperature, and nutrient availability [31]. Therefore, it is believed that marine microbes are both taxonomically diverse and metabolically complex, providing a vast resource for mining novel genes and biocatalysts. Enzymes from marine microbes are likely to have a range of quite diverse biochemical and physiological characteristics that have allowed the microbial community to adapt and ultimately thrive in these unfavorable conditions [52]. Recently, various novel lipases and esterases have increasingly been identified from seawater to marine sediment microbial community, for example, cold-active lipase Lip1 from *Pseudoalteromonas haloplanktis* TAC125 [8], esterase EstA from seawater metagemomic library [6], low-temperature-active lipase h1Lip1 [21], cold-adapted alkaline esterase EM2L8 from deep-sea sediment metagenome [45], OLEI01171 from the oil-degrading marine bacterium *Oleispira antarctica*, RhLip from Arctic marine bacterium *Rhodococcus* sp. AW25M09 [9] and EstB from marine microorganism *Alcanivorax dieselolei* B-5(T) [59]. Among these identified lipolytic enzymes, cold-adapted enzymes have been paid great attentions for their economic benefits through energy savings [5]. Since the marine sediments largely represent low-temperature environments, the presence of low-temperature-adapted bacteria with low-temperature-active enzymes are highly expected [21].

In our previous study, we constructed a fosmid metagenomic library IMCAS-F003 from South China Sea marine sediment microbial DNA, and the genetic information contained in the library was analyzed by large scale fosmid end sequencing [27]. In the present work, a novel low-temperature-active alkaline esterase Est12 was identified from this library, and the structure and function of Est12 were investigated. Our study sheds new lights on better understanding the lipolytic enzymes of marine origin and provides a potential biocatalyst for future industrial application.

Materials and methods

Lipolytic activity clones screening

To screen for lipolytic activity clones, the library IMCAS-F003 we previously constructed was plated on LB agar medium supplemented with 1 % tributyrin [45] and 12.5 μg mL^{-1} chloramphenicol. Lipolytic activity clones were identified by the formation of clear zones around colonies after incubation for 24–48 h at 30 °C.

Fosmid sequencing and sequence analysis

Fosmid pFL12 was purified by using Plasmid Mini Kit I (Omega, Doraville, GA), and mechanically sheared DNA of 1.5–3 kb was ligated to pUC118 vector for shotgun sequencing. The sequence coverage was above tenfold, and the resulting DNA sequences were assembled using Lasergene package, version 7.10 (DNA star, USA). After sequence assemblage, two contigs of 8.8 and 16.5 kb, respectively, were obtained. The gap between the two contigs was closed by primer-walking method. Open reading frame (ORF) analysis was performed using Glimmer version 3.02 [10]. The predicted function of ORFs was annotated using BlastX search toward the NCBI nonredundant protein database and finalized by manual inspection. Promoter prediction was carried out by using Softberry (http://linux1.softberry.com/all.htm) and NNPP version 2.2 (http://www.fruitfly.org/seq_tools/promoter.html). The prediction of signal peptide was performed with the help of SignalP 3.0 server [4]. Multiple sequence alignments were carried out by Clustal X, version 1.83 [54]. Phylogenetic and molecular evolutionary analyses were conducted by the neighbor-joining method using MEGA version 4 [53]. Bootstrapping [15] was used to estimate the reliability of phylogenetic reconstructions (1000 replicates).

Expression and purification of Est12

For the overexpression of Est12, the full length of orf14 was amplified using the original fosmid pFL12 as template with primers: 5′-GGAATTC*CATATG*GCG TTGTTTCAGTGCG-3′, 5′-CCC*AAGCTT*TCACGCAGGC GCTGTTCCCG-3′.

The Nde I and Hind III restriction enzyme sites were underlined in the forward and reverse primers. The PCR product was digested by Nde I and Hind III, and the product was purified and cloned into an expression vector, pET-28a (+), and the recombinant plasmid was transformed into *E. coli* BL21 (DE3) competent cells.

When cells were grown to an OD_{600} of 0.5 at 37 °C in LB medium containing 34 μg/mL kanamycin, 0.5 mM

isopropyl β-D-1-thiogalactopyranoside (IPTG) was added to induce the recombinant protein. After further growth for 3 h, the cells were harvested by centrifugation at 6500 g for 20 min at 4 °C. The cell pellet was then resuspended in lysis buffer (50 mM Na-phosphate pH 8.0, 300 mM NaCl, 5 % glycerol (v/v), 2 mM 2-mercaptoethanol) and homogenized by ultrasonication on ice. The lysate was centrifuged for 30 min at 12,000 g at 4 °C. The supernatant-containing soluble Est12 protein was then applied onto Ni–NTA resin (QIAgen) as described by Liu et al. [40]. The eluate of Est12 protein was further purified on a superdex 200 column by ÄKTA prime plus (GE) equilibrated with Tris–HCl buffer (50 mM Tris–HCl pH 7.8, 300 mM NaCl, 1 mM EDTA, 5 % glycerol (v/v), 2 mM 2-mercaptoethanol). The fraction-containing Est12 was concentrated to 100 mg/mL using an Amicon concentrator 10 kDa (Millipore), and the protein concentration was determined using Bradford assay with BSA as standard. Lastly, Est12 was stored at −80 °C prior to crystallization attempts.

Enzymatic activity assay

Activity was measured using *p*-nitrophenyl (NP) esters as substrates [38]. The standard reaction mixture contained 0.01 mL of 10 mM substrate in acetonitrile and 0.98 mL of 50 mM of Tris–HCl (pH 8.0) buffer containing 0.1 % arabic gum and an appropriate amount of the enzyme in a final volume of 1 mL. Unless otherwise specified, the activity of enzyme was determined at 40 °C for 5 min by measuring the absorbance of liberated *p*-NP at 410 nm. The background hydrolysis of the substrate was deduced using a reference sample of composition identical to the reaction mixture but with no enzyme added. Measurements were carried out for at least three times. One unit (U) of enzyme activity was defined as the amount of enzyme required to release 1 μM of *p*-NP per minute under the assay conditions. The kinetic constants K_m and V_{max} of Est12 using *p*-NP caproate as a substrate were calculated from the Lineweaver–Burk plot.

Biochemical properties of Est12

Substrate specificity was determined at 40 °C and pH 9.0 toward *p*-NP esters with chain lengths ranging from C_2 to C_{16}. The optimum temperature was investigated in the range of 5–65 °C with 5 °C intervals. The effects of pH on hydrolysis activity were examined over the range of pH 5.0–11.0, and the buffers used were citrate buffer (pH 5.0–6.0), sodium phosphate buffer (pH 6.0–8.0), Tris–HCl buffer (pH 8.0–9.0), and sodium bicarbonate buffer (pH 9.0–11.0). The thermostability of the esterase was examined by incubating the enzyme in 50 mM Tris–HCl buffer (pH 9.0) at 40, 50, and 60 °C, and the relative activities were measured every 10 min for 1 h for each temperature using the standard assay.

The effects of divalent metal ions on enzyme activity were determined using metal salts ($CaCl_2$, $CoCl_2$, $CuCl_2$, $ZnCl_2$, $MnCl_2$, $MgCl_2$, and $NiCl_2$) at final concentrations of 5 mM. The effects of inhibitors on esterase activity were examined using diethyl pyrocarbonate (DEPC), phenylmethylsulfonyl fluoride (PMSF), ethylene glycol-bis (β-aminoethyl ether)-*N*, *N*, *N*′, *N*′-tetraacetic acid (EGTA), ethylenediamine-tetraacetic acid (EDTA), 2-merchaptoethanol (2-ME), and dithiothreitol (DTT) at final concentrations of 5 mM. The effects of detergents on esterase activity were examined using sodium dodecyl sulfate (SDS), Tween 20, Tween 80, cetyltrimethyl ammonium bromide (CTAB), and Triton X-100 at final concentrations of 0.2–5 %. The effects of organic solvents on esterase activity were examined using dimethyl sulfoxide (DMSO) and dimethylformamide (DMF) at final concentrations of 1–10 %, methanol, ethanol, and acetone at final concentrations of 10–40 %. All the tests were performed using the standard assay, and the activity of the enzyme without additives added in the reaction mixture was defined as 100 %.

Protein crystallization

The diffraction-quality crystals were obtained at 277 K by mixing 1.5 μl reservoir solution consisting of 0.3 M Magnesium chloride hexahydrate, 0.1 M Tris hydrochloride pH8.5, 24 % w/v PEG4000 with an equal volume of 5 mg/mL of the protein solution by the hanging drop. The crystals were typically shaped like diamonds. The cry-protectant solution was mother solution plus 15 % glycerol.

Data collection and structure determination

The diffraction data were collected using an MX225 CCD detector at 100 K on beamline BL17U1 of Shanghai Synchrotron Radiation Facility (SSRF) of China. The raw data were reduced and scaled using the HKL2000 software package [44]. Data collection and reduction statistics are summarized in Table 1. The crystal belonged to the space group *C2* with approximate unit-cell parameters $a = 133.4$, $b = 63.8$, $c = 88.7$ Å, $\alpha = 90$, $\beta = 127.1$, $\gamma = 90^{o}$. The structure was solved by molecular replacement by Phaser [42] from the CCP4 suite [57] with estA of *Streptococcus pneumonia* (PDB code 2UZ0) which had 40 % identity with Est12 as a search model. The estA structure contained two molecules in the asymmetric unit. After one round of rigid-body refinement with Phenix [1], manual rebuilding was performed in Coot [12]. Subsequently, further rounds of restrained refinement were performed and waters were added and adjusted. Figures containing protein structures were generated with PyMol (www.pymol.org).

Table 1 Data collection and refinement statistics for Est12

X-ray statistics	Est12
Data collection	
Space group	*C*2
Unit-cell parameters	$a = 133.4$, $b = 63.8$, $c = 88.7$ Å $\alpha = 90$, $\beta = 127.1$, $\gamma = 90$ °
Molecules in asymmetric unit	2
Wavelength (Å)	1.0001
Resolution (Å)	35.07–1.39
R_{merge} (%)	10.3 (48.6)
Mean I/σ (I)	16.2 (3.1)
Completeness (%)	99.8 (99.8)
Multiplicity	6.7 (6.1)
Refinement	
No. of reflections	101,251
R_{work}/R_{free} (%)	17.56/18.13
No. of atoms	
Protein	3758
Ligand/ion	–
Water	644
R.m.s.d	
Bond lengths (Å)	0.007
Bond angles (°)	1.19
Ramachandran statistics (%)	96.7
Allowed	3.3
Disallowed	0

Nucleotide sequence and PDB entries

The nucleotide sequence of the fosmid pFL12 has been deposited in GenBank with an accession number of FJ483464. The PDB number of Est12 was 4RGY.

Results and discussion

Lipolytic activity-based screening of fosmid library

The metagenomic fosmid library used for screening was constructed from deep-sea sediment community, South China Sea, with a water depth of 778.5 m. The in situ temperature of the sampling sediment was around 4 °C; thus, cold-adapted enzymes were expected. Here, the library was screened for lipolytic activity on tributyrin agar plates, and a positive clone, pFL12, was selected. This clone showed relatively high hydrolysis activity on plate at low temperature compared to other clones. When stored at 4 °C for one week, the clear zone around the colony was about five to six times larger in size than that stored for three days (data not shown).

Genetic information on the pFL12 fosmid clone

The fosmid clone pFL12 was randomly shotgun sequenced. The sequencing result indicated that this clone contained a 26139-bp foreign DNA fragment with a relative high G + C content (65 %). A total of 17 ORFs were found out by using Glimmer (Electronic Supplementary Material 1), of which 9 proteins showed very low identity (less than 35 %) with their hits, and only 3 proteins displayed higher identity of >50 %. The enzyme in the database that was the most similar (78 % identity) to our proteins (orf13) was a sulfatase from an uncultivated bacterial symbiont of the marine sponge *Theonella swinhoei*. Since the insert DNA did not carry any phylogenetic marker genes, its microorganism of origin was not really known. However, considering the low identity of the genes on the DNA fragment, it is probably from a hitherto unknown or uncultured marine microorganism.

Interestingly, besides orf13, orf7 encoded another sulfatase with 32 % identity to that from *Bacteroides thetaiotaomicron*VPI-5482. Sulfatases, belonging to hydrolase superfamily, catalyze the hydrolysis of a diverse range of sulfate ester substrates, including hydrophobic glucosinolate, steroid, and thyronine sulfates. These enzymes in prokaryotes typically function as scavengers, removing sulfate groups from exogenous substrates to provide sulfur sources for their hosts, or as the first step in their mineralization [22]. Therefore, we speculated that this DNA fragment is originated from the microorganism involved in sulfur cycle in marine sediment environment.

One of these predicted ORFs encodes a 270-amino-acid protein (named Est12) showing the highest identity of 64 % with putative esterase from *Geobacillus* sp. Y412MC10. Further expression and characterization were focused on this protein.

Sequence analysis of Est12

A putative promoter region of Est12 by the presence of -35 region, GTGAAT, -10 region, TATACT, and a putative ribosomal binding site, AGGAGA, 8 bp upstream of the ATG initiation codon were identified. Analysis of RNA secondary structure indicated that a region downstream of the termination codon TGA tend to form stable stem-loop structure, which was probably a rho-independent transcription terminator (Electronic Supplementary Material 2). The G + C content of this ORF was 66 %, which was almost identical to 65 % of the whole fosmid inserted DNA. No potential signal sequence was detected in this protein, as revealed by the SignalP program.

Lipases and esterases contain the conserved active site motif of the pentapeptide Gly-x-Ser-x-Gly with a serine acting as the catalytic nucleophile, a conserved aspartate or glutamate

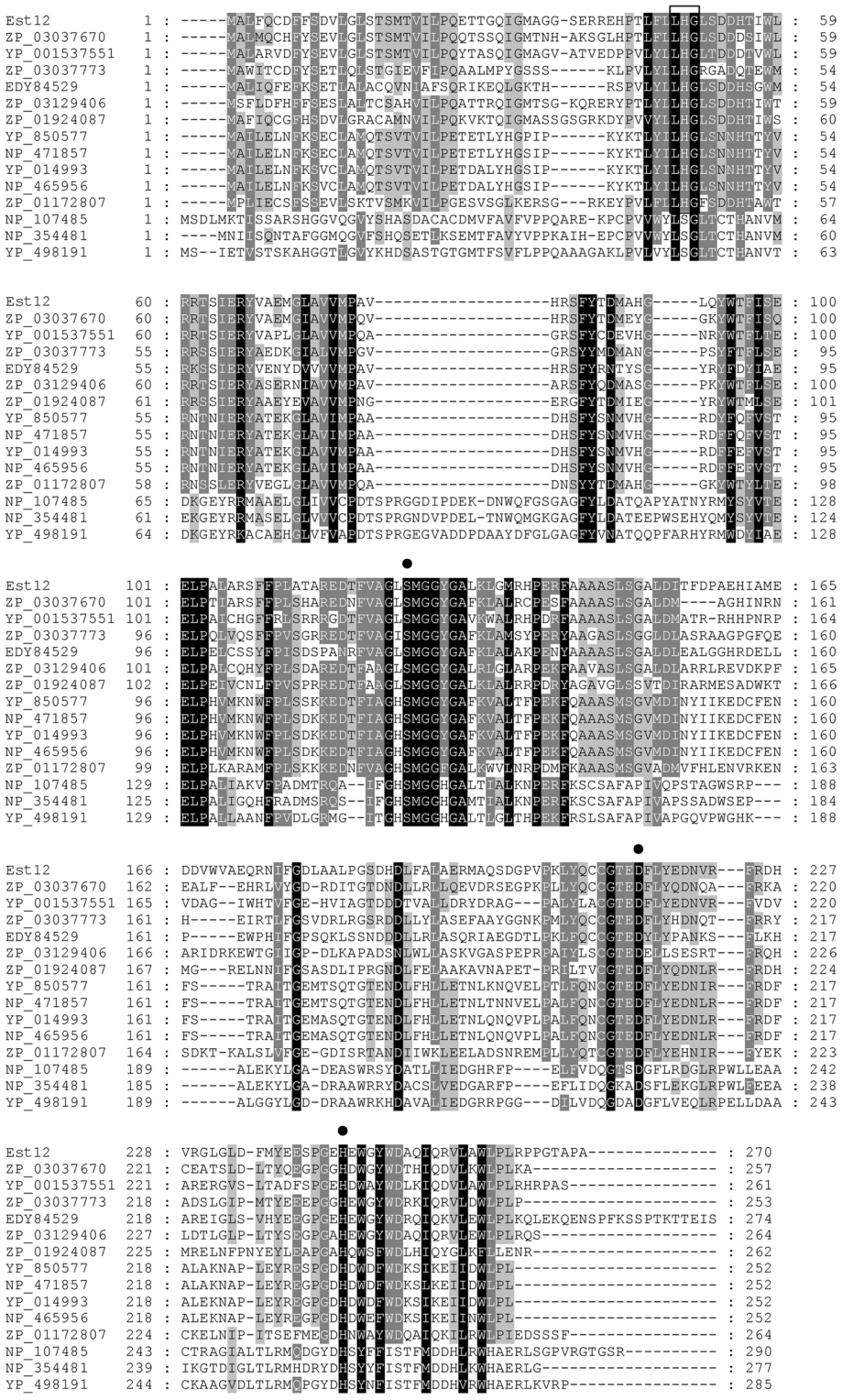

Fig. 1 Sequence alignment of Est12 with its closest members and three representative members of family EstA. The aligned sequences are as follows: esterase Est12 (this study); putative esterase of *Geobacillus* sp. Y412MC10 (GenBank accession no. ZP_03037670); putative esterase of *Salinispora arenicola* CNS-205 (ZP_001537551); putative esterase of *Geobacillus* sp. Y412MC10 (ZP_03037773); putative esterase of *Verrucomicrobiae bacterium* DG1235 (EDY84529); putative esterase of *Chthoniobacter flavus* Ellin428 (ZP_03129406); putative esterase of *Victivallis vadensis* ATCC BAA-548 (ZP_01924087); tributyrin esterase of *Listeria welshimeri serovar 6b* str. SLCC5334 (YP_850577); hypothetical protein lin2527 of *Listeria innocua* Clip11262 (NP_471857); tributyrin esterase of *Listeria monocytogenes* str. 4b F2365 (YP_014993); hypothetical protein lmo2433 of *Listeria monocytogenes* EGD-e (NP_465956); hypothetical protein B14911_15770 of *Bacillus* sp. NRRL B-14911 (ZP_01172807); esterase of *Mesorhizobium loti* MAFF303099 (NP_107485); esterase D of *Agrobacterium tumefaciens* str. C58 (NP_354481) and carboxylesterase of *Novosphingobium aromaticivorans* DSM 12444 (YP_498191). The putative catalytic triad (Ser125, Asp215, and His244) on Est12 deduced from the sequence alignment is indicated by *solid circle*. Putative motif involved in the formation of the oxyanion hole is *boxed*. The alignment was obtained using the Clustal X program

and a histidine, together constituting a catalytic triad, organized in the hydrolase fold [3]. Sequence alignment revealed that Ser125, Asp215, and His244 of Est12 probably composed the typical catalytic triad Ser-Asp-His with the active site serine in the consensus sequence Gly-Leu-Ser-Met-Gly (Fig. 1).

A phylogenetic tree was constructed for Est12, and its closest blast matched members and representative members of formerly reported eight lipolytic enzyme families, three new families [3, 6, 32, 35]. The result showed that Est12 and its closest members formed a separate group

related to EstA family (Fig. 2). The relationship between Est12 and EstA as revealed by the comparisons of amino-acid sequences showed that the former displayed a very low similarity with representative members of EstA with the highest identity of 26.5 and 25.7 % to esterase from *Aurantimonas* sp. SI85-9A1 (ZP_01228660) and *Hoeflea phototrophica* DFL-43 (ZP_02167917), respectively. Furthermore, the sequence patterns conserved around the putative active site residues as well as several other blocks of Est12 group were different from those of EstA representative members. The remarkable difference between the two families was that a gap of 19 amino acids appeared in members of Est12, thus making them about 20 amino acids shorter in length than the EstA family. Based on these data, we proposed that Est12 together with its closest members represented a new family or subfamily of bacterial lypolytic enzymes.

Substrate specificity of recombinant Est12

The complete ORF of Est12 was amplified by PCR and cloned into pET28a(+) using *E. coli* BL21 (DE3) as host, and the resulting protein was purified. The substrate specificity of the purified enzyme was investigated by using various chain lengths of *p*-NP esters (C_2–C_{16}) at 40 °C and pH 9.0 (Fig. 3a). The result showed that Est12 exhibited the highest activity toward *p*-NP caproate (212 ± 9.6 U/mg). The kinetic constants of Est12 using *p*-NP caproate as a substrate were determined as K_m = 0.39 mM, k_{cat} = 3.35 × 10^2 s^{-1}, and k_{cat}/K_m = 8.6 × 10^2 mM^{-1} s^{-1}. High hydrolysis activity was also obtained with other short- and middle-chain *p*-NP esters, such as *p*-NP butyrate (approx. 80 %) and *p*-NP caprylate (approx. 40 %), but very low activity was observed with longer chain *p*-NP esters. Lipases, by definition, have the ability to hydrolyze long-chain fatty acids esters ($\geq C_{10}$), whereas esterases hydrolyze ester substrate with short-chain fatty acids esters ($\leq C_{10}$) [55]. The Est12 identified here preferred short- and middle-chain *p*-NP esters as substrate with the highest hydrolysis activity toward *p*-NP caproate (C_6), which indicated that Est12 was an esterase.

Optimum temperature, thermostability, and effects of pH on enzyme activity

Est12 displayed high activity in a temperature range of 40 °C–55 °C with its highest activity at 50 °C by using *p*-NP caproate as substrate (Fig. 3b). This result revealed that esterase Est12 exhibited a relatively high optimum temperature, though it originated from the microbe in cold environment (deep-sea sediment). However, comparing with the maximal activity at 50 °C, the enzyme remained 48, 53, and 68 % activity at low temperatures 5, 15, and 25 °C, respectively. Moreover, thermostability analysis indicated that the activity of Est12 decreased by more than 80 % after 60 min at 50 °C, and the enzyme was rapidly inactivated with only 12 % relative activity remained at 60 °C after 10 min (Fig. 3c). These results demonstrated that Est12 was low-temperature active and thermolabile, both of which were typical features of cold-adapted enzymes [14]. Considering these, we suggested that Est12 was a low-temperature-adapted esterase. In addition, the optimum activity of Est12 occurred at an alkaline pH 9, which was about two times higher than that at pH 7.0 (Fig. 3d). This suggested that Est12 was an alkaline-tolerable esterase.

Recently, several novel esterases have been identified from metagenomic library of different marine environment such as surface sea water [6, 13], intertidal zone sediments [18], and deep-sea sediments [17, 26, 29, 46], which are summarized in Table 2. It is noticed that Est12 has broad temperature tolerance ability, with a 50 % of optimal activity retained ranging from 10 to 60 °C. It is outstanding compared with other marine-derived esterase, most of which can tolerant temperature variation of no more than 35 °C. The wide temperature compatibility of Est12 will broaden its application in terms of different process temperature required. In addition, Est12 appears to possess high alkaline tolerance, with 80 % of optimal activity maintained under pH up to 10, which is similar to EstF, another esterase originated from the same deep-sea marine sediment reported previously. While the majority of the marine-derived esterase works under a pH below 9, Est12 and EstF are unique in terms of their alkaliphilic property, which could be applied in many esterase-associated industrial processes performed under alkaline environment [34].

Effects of metal ions and inhibitors on enzyme activity

The effects of metal ions and inhibitors on enzyme activity were determined by using various ions and inhibitors at a concentration of 5 mM (Table 3). It was shown that Est12 was sensitive to Cu^{2+} and Zn^{2+}, and the enzyme activity was not significantly affected by Ni^{2+}. The strong inhibitions by Zn^{2+} also exhibit in other esterase [18]. However, the structure basis for the inhibition has not been stated in previous literature and cannot be explained in our Est12 structure as well. Co^{2+}, Ca^{2+}, Mn^{2+}, and Mg^{2+} increased the activity in different degrees, and Ca^{2+} was especially as an activator, increasing the activity to about 151 % compared with that without ions addition. The enzyme activity was inhibited by all inhibitors used, and strongly inhibition was observed in the presence of EGTA as the chelator of Ca^{2+} (Table 4). This result further confirmed that the enzyme activity

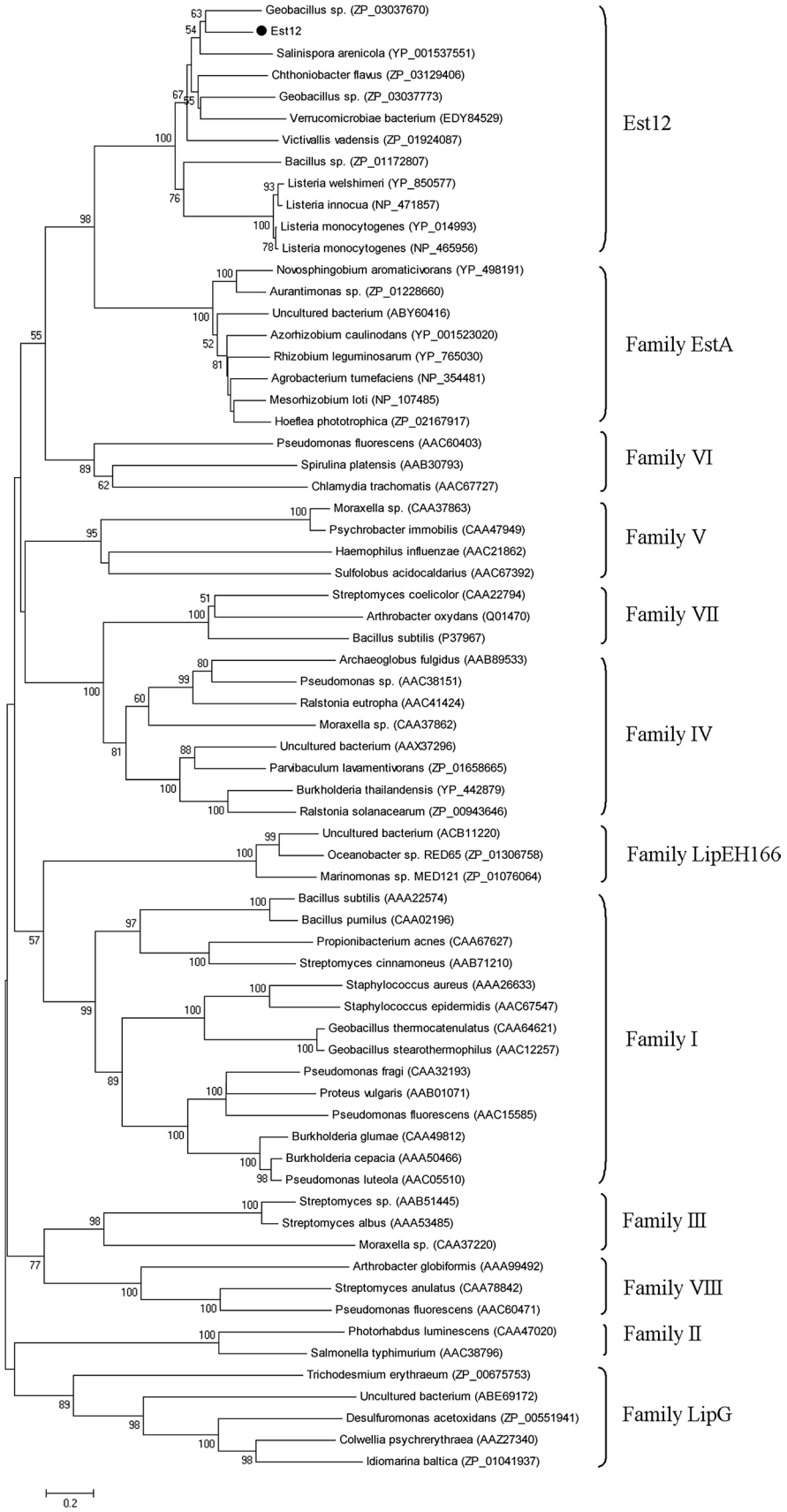

Fig. 2 Phylogenetic tree of Est12 (*solid circle*) and other lipolyitc enzymes. The tree was constructed by using neighbor-joining method for calculation using MEGA (version 4) software. Analysis was bootstrapped, and the values higher than 50 are indicated at respective nodes (1000 replications). The enzymes belonging to different families were referred to published data [3] and retrieved from Genbank. Amino-acid sequences were aligned by Clustal X (version 1.83). The length of the branches indicates the divergence among the amino-acid sequences. Scale bar corresponds to 20 % estimated sequence divergence

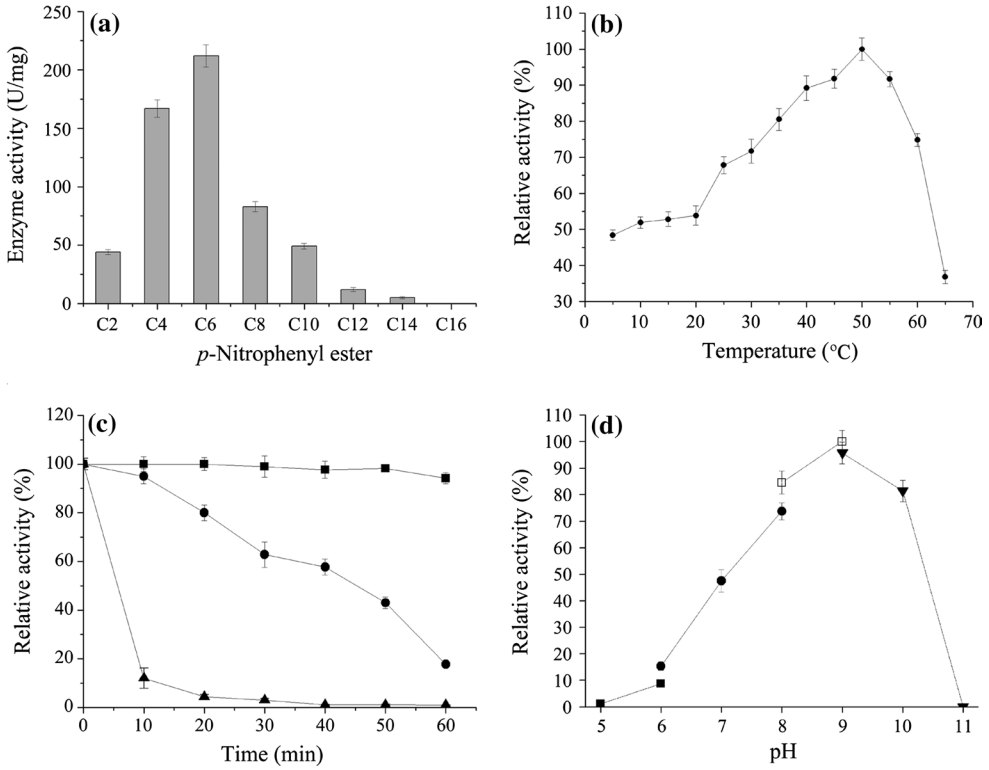

Fig. 3 Biochemical features of esterase Est12. **a** Substrate specificity of Est12. Hydrolytic activity was determined toward different chain length of *p*-nitrophenyl (NP) esters: acetate (C_2), butyrate (C_4), caproate (C_6), caprylate (C_8), caprate (C_{10}), laurate (C_{12}), myristate (C_{14}), and palmitate (C_{16}). The highest activity, observed with the caproate (C_6), was 212 ± 9.6U/mg. **b** Effects of temperature on Est12 activity. The enzyme activity was measured toward *p*-NP caproate at various temperatures at pH 9.0. **c** Effects of temperature on Est12 stability. The enzyme was incubated at 40 °C (*solid square*), 50 °C (*solid circle*), and 60 °C (*solid triangle*) for the indicated periods of time, and residual activity was measured using the standard assay. Activity before incubation was defined as 100 %. **d** Effects of pH on the esterase activity of Est12. Buffers used were citrate buffer (*solid square*) for pH 5.0–6.0, sodium phosphate buffer (*solid circle*) for pH 6.0–8.0, Tris–HCl buffer (*square*) for pH 8.0–9.0, and sodium bicarbonate buffer (*solid inverted triangle*) for pH 9.0–11.0. The Est12 activities for (**a**), (**b**), and (**d**) were measured by incubating for 5 min

Table 2 Biochemical characteristics of esterase from different metagenomic libraries of different marine environments

Enzyme	Environment origin	Temperature (°C) (optimum)[a]	pH (optimum)[b]	Substrate (optimum)[c]	Reference
Est9x	Surface seawater	50–75(65)	7.0–9.0(8.0)	C_2–C_6(C_2)	Fang et al. [13]
EstB	Surface seawater	35–50(45)	6.5–7.5(7.5)	C_4–C_6(C_4)	Chu et al. [6]
Est_p1	Neritic sediments	25–45(40)	6–9(8.6)	C_4	Peng et al. [46]
EstF	Deep-sea marine sediment	25–60(50)	8–10(9)	C_2–C_4(C_4)	Fu et al. [17]
FLS18D	Deep-sea marine sediment	30–50(50)	7–9(8)	C_4–C_6 (C_4)	Hu et al. [27]
EstA	Surface seawater	30–50(45)	5.5–7.5(6.5)	C_4–C_6(C_6)	Chu et al. [6]
Est97	Intertidal zone sediment	20–45(35)	7–9.5(7.5)	C_4–C_6(C_6)	Fu et al. [18]
Est12	Deep-sea marine sediment	10–60(50)	8–10(9)	C_4–C_6(C_6)	This study

[a] The temperature range is the temperatures at which the activities are at least 50 % of the maximum activity

[b] pH range is the pHs at which the activities are at least 50 % of the maximum activity

[c] Substrates' ranges are the *p*-nitrophenyl esters at which the activities are at least 50 % of the maximum activity

was dependent on Ca^{2+}. Some Ca^{2+}-dependent esterase identified had a Ca^{2+}-binding GXXGXD motif in their sequence, which played an important role in enzyme activity and thermostability [48, 51]. However, there is not the Ca^{2+}-binding motif in the sequence of Est12. Therefore, in the other hand, the mechanism of Ca^{2+} as

Table 3 Effects of metal ions on the esterase activity of Est12

Metal ions	Relative activity (%)
Co^{2+}	130 ± 8
Ca^{2+}	151 ± 12
Mn^{2+}	142 ± 6
Mg^{2+}	123 ± 9
Ni^{2+}	96 ± 6
Zn^{2+}	33 ± 4
Cu^{2+}	13 ± 3

Table 4 Effects of inhibitors on the esterase activity of Est12

Inhibitors	Relative activity (%)
DEPC	34 ± 4
PMSF	25 ± 1
EGTA	29 ± 3
EDTA	82 ± 7
2-ME	70 ± 6
DTT	50 ± 3

an activator has one more probability. For instance, Kim et al. [33] reported that Ca^{2+} ion in the EstA did not directly involve in the catalysis of the enzyme but played a critical role in maintaining its stability under physiological condition.

Inhibitors, DEPC, and PMSF markedly influenced the enzyme by reducing the activity to 34 and 25 %, respectively, while EDTA and 2-ME gave a lower inhibition of the enzyme activity (Table 4). PMSF and DEPC are specific modifiers of serine proteases and histidine residues, respectively, suggesting the involvement of a histidine and a serine at the active site of the enzyme.

Effects of detergents and organic solvents on enzyme activity

The effect of detergents on Est12 activity was examined by addition of SDS, Tween 20, Tween 80, CTAB, and Triton X-100 with concentrations from 0.2 to 5 % (Table 5). Est12 was very sensitive to even low concentration (0.2 %, w/v) of SDS and CTAB. Addition of 0.2 % (w/v) Tween 20, Tween 80, and Triton X-100 decreased the enzyme activity to 84, 84, and 56 %, respectively. The enzyme activity was almost completely inactivated with 5 % concentration of Tween 80 and Triton X-100. Based on these results, Est12 seemed not stable in the presence of most detergents tested. The effects of organic solvents on Est12 activity were determined using DMSO and DMF at concentrations of 1 to 10 %, and methanol, ethanol, and acetone at concentrations of 10 to 40 % (Table 6). The

Table 5 Effects of detergents on the esterase activity of Est12

Detergents	Relative activity (%) at concentration (w/v) of (%)		
	0.2	1	5
SDS	2 ± 1	0	0
Tween20	84 ± 6	64 ± 6	25 ± 4
Tween80	84 ± 8	47 ± 3	7 ± 1
CTAB	0	0	0
Triton X-100	56 ± 4	47 ± 9	7 ± 3

enzyme activity was not significantly affected in the presence of 1 to 5 % concentration of DMSO or 1 % concentration of DMF, while with the concentration increased, the enzyme seemed more tolerable to DMSO than DMF. Moreover, in the presence of 10 % concentration of methanol, ethanol and acetone, 80, 53 and 61 % relative activity remained, respectively. Furthermore, Est12 exhibited 14 % activity remained at even 40 % concentration of methanol; however, the same concentration of ethanol or acetone inactivated Est12 activity completely. Taken together, Est12 was relatively stable in low concentration of organic solvents, and it showed the best tolerance to methanol, which is an important property for industrial applications.

Overall structure of Est12

The 1.39 Å resolution crystal structure of Est12 was further determined in space group $C2_1$ by molecular replacement using the *Streptococcus pneumonia* estA (PDB code 2UZ0) as initial model. The crystallographic statistics for data collection and structure refinement are summarized in Table 1. The R factor of the present model was 0.16, with an R free of 0.18. The asymmetric unit contained two identical molecules. Gel-filtration experiment showed that the protein purified had a molecular weight of approximately 66 kDa against of which the monomer was about 30 kDa according to the amino-acid residues. Collectively, it can be concluded that Est12 is dimerized in the native state. Additionally, each monomer was perfectly superimposable and displayed a marginally ellipsoidal shape as shown in Fig. 4a.

The Est12 monomer had a large catalytic domain which exhibited a characteristic α/β hydrolase topology. The fold consisted of repeating motifs that form a central, predominantly parallel (except β2) eight-stranded β-sheet surrounded on either side by α-helices. The prototypic catalytic triad was further identified as Ser125, Asp215, and His244. Ser125 was located in the apex of nucleo-philic elbow between β5 and α5, within the conserved GXSXG motif, which was a signature sequence for the hydrolase

Table 6 Effects of organic solvents on the esterase activity of Est12

Organic solvents	Concentration (v/v) (%)	Relative activity (%)
DMSO	1	100 ± 5
	5	98 ± 4
	10	74 ± 5
DMF	1	101 ± 3
	5	72 ± 7
	10	43 ± 3
Methanol	10	80 ± 6
	20	64 ± 9
	40	14 ± 3
Ethanol	10	53 ± 3
	20	27 ± 3
	40	0
Acetone	10	61 ± 6
	20	18 ± 4
	40	0

family. His244 was located on the loop between β8 and α9, and Asp215 was located between β7 and α8 (Fig. 4b). As shown in Fig. 4b, the three amino acids in the catalytic triad were located in proximity. The hydrogen bond interaction network contributed to the stabilization of this conformation, with distances of 2.39 Å from Ser125 O^{γ} to His 244 $N^{\varepsilon 2}$ and 2.8 Å from His244 $N^{\delta 1}$ to Asp215 $O^{\delta 2}$ (Fig. 4b).

Inspection of the solvent accessible surface revealed the presence of a long and narrow cavity, delimited by residues Gly50, Ser52, Asp53, Ile57, Arg61, Leu124, and Trp246, which spanned from the protein surface to the catalytic Ser125. The catalysis mechanism of Est12 might be defined as the traditional esterase, in which Ser125 represented as the catalytic nucleophile, His244 activates the serine, and Asp215 makes a hydrogen bond with His244 thus completing the catalytic triad. During the catalysis process, the oxyanion hole played an important role in ester hydrolysis through the activation of the substrate carbonyl group for attack and stabilization of the negative charge of tetrahedral intermediate. After comparing the crystal structure of Est12 with other esterase such as estA and, OLEI01171, the oxyanion hole of Est12 might be composed of Leu51 and Met126 (Fig. 4b).

Structure comparison with other esterases

A structural fold similarity search using DALI identified several proteins with structural homology to Est12 [25]. The structure of Est12 was most similar to estA from *Streptococcus pneumonia* (PDB ID code 2UZ0; *Z*-score = 34.2, r.m.s.d. = 1.39 Å for 245 residues) [33] and OLEI01171 from *Oleispira Antarctica* (PDB ID code 3s8y; *Z*-score = 29.4, r.m.s.d. = 1.7 Å for 277 residues) [37]. Structure-based sequence alignment showed that the sequence identities of Est12 with estA and OLEI01171 were 40 and 22 %, respectively, and 31 residues are completely conserved, including the catalytic residues of Ser125 and His244 (Fig. 5). Structure comparison indicated that Est12 resembles most parts of its structure to estA and OLEI01171, but the most striking difference between these proteins is the cap domain (Fig. 6a), which could play important roles in substrate specificity among these esterases. As shown in Fig. 6b, the cap domain of Est12 consists of an α-helix and a flexible region, which prefers *p*-NP with C_6 and C_4, though C_8 as well as even C_{10} and C_2 are also accessible (Fig. 3a). The cap domain of estA was composed of an α-helix and a 3_{10} helix (Fig. 6c); thus, it could only hydrolyze *p*-NP with C_4. Unlike Est12 and estA, the cap domain of OLEI01171 formed longer but narrower

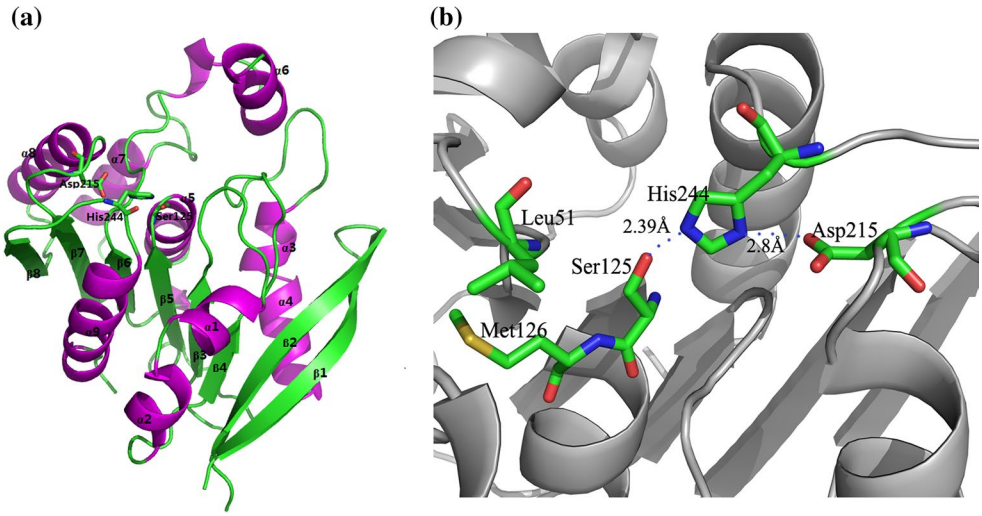

Fig. 4 Structural characterization of the Est12 protein. **a** The Est12 monomer structure. α-helices and β-sheets were shown in *magenta* and *green*, respectively, and Ser125, Asp215, and His244 were shown in sticks. **b** The catalytic site consisting of three residues Ser125, Asp215, and His244, as well as the oxyanion hole residues Leu51 and Met126, were shown in sticks

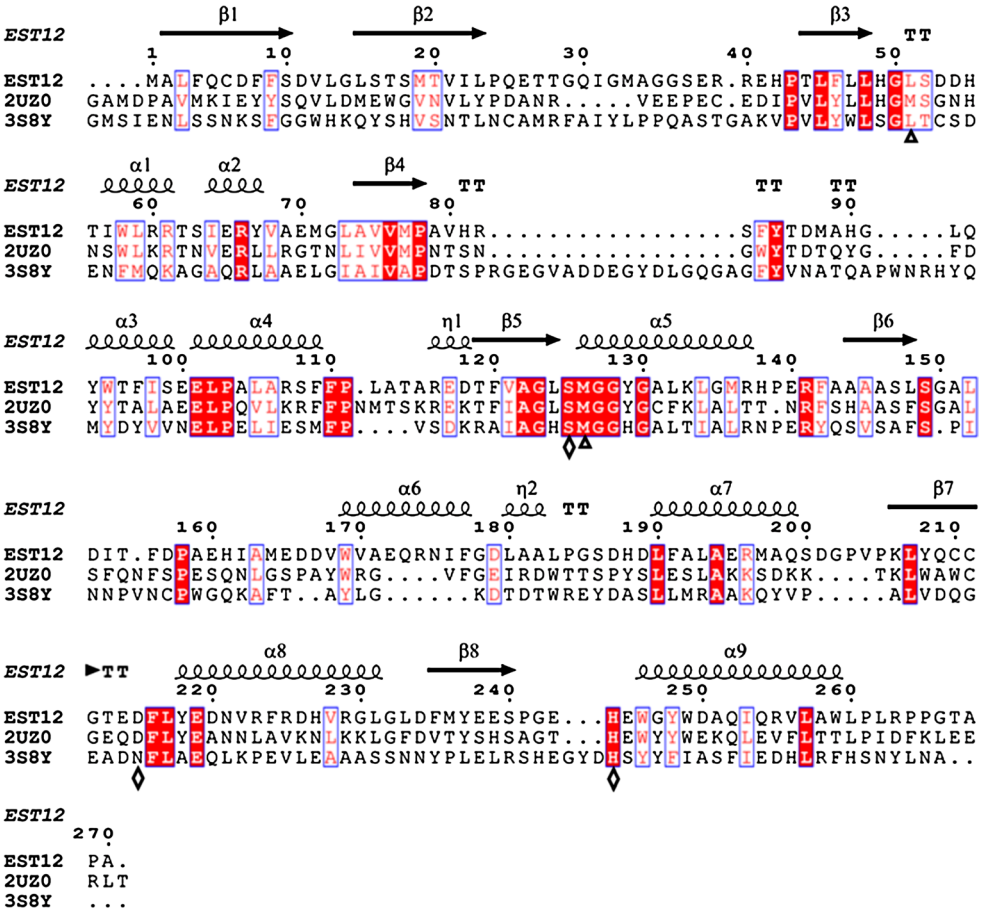

Fig. 5 Sequence alignment of Est12 and other esterase. The catalytic triads (Ser125, Asp215, and His244) were shown as diamond and the oxyanion holes (Leu51 and Met126) were shown as *triangle*. Sequence alignments were assembled using ClustalX2 and visualized using ESPript software, both located on the ExPASy Proteomics Server (http://au.expasy.org/)

channel (Fig. 6d), which resulted in a restrained substrate accessibility so that only short acyl-chain (C_2) was suitable [37]. It also suggests that the esterase could hydrolyze longer carbon chain when its cap domain was more expansive and flexible, which was consistent with previous reports [43, 49].

Cold-active enzymes could be more useful for food and agricultural applications than their counterparts because of higher catalytic abilities at lower temperatures. The thermostability of lipolytic enzymes is regarded to be one of the most important characteristics for biotechnological applications [30]. Est12 was identified as a new cold-active esterase, with 48 % of maximum activity retained at 5 °C (Fig. 3b). It has been known that cold-active enzymes have evolved many structural features that confer a high level of flexibility. For instance, the active catalytic triads are shielded by a mobile cap domain, whose open position determines the active conformation of the esterase [30]. This flexible feature in cap domain was also observed in Est12, which might partly contribute to its cold adaption. Additionally, the increase of local mobility by Gly residues around the active site and more Ser and Met may contribute to systemic cold adaptation. Gly residues, which are unconstrained in loops, increase conformational freedom of the native state and Ser residues can weaken hydrophobic clusters to increase flexibility. Met residues contribute to flexibility via their high degree of freedom and lack of branching and charge or dipole interactions [19, 50]. Here, in the case of Est12, the percentage of Gly (8.5 %), Ser (5.5 %), and Met (4 %) are relatively higher than those observed for other amino-acid residues. The flexible cap domain and relatively high percentage of Gly, Ser, and Met entitled Est12 to function under low temperature.

Conclusions

Est12 was a novel low-temperature-active, broad temperature-compatible, and methanol and alkaline-tolerable esterase. The crystal structure of Est12 shows a typical α/β hydrolase domain as well as a flexible cap domain which may responsible for the relatively wide spectrum of substrate and its cold-active feature. In addition, the relatively high percentage of Gly, Ser, and Met in Est12 may also contribute to its cold adaption. These results provide some structure–function relationship of esterase. Furthermore,

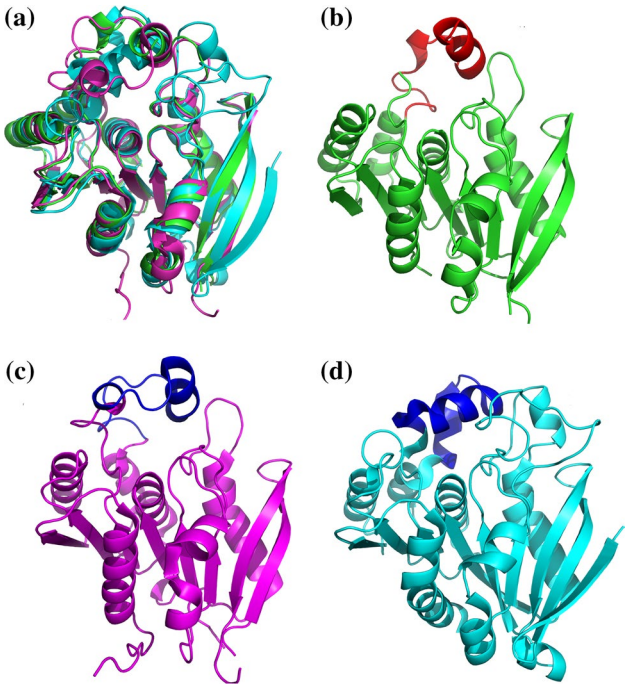

Fig. 6 Structure comparison of Est12 with other esterase. **a** Comparison of Est12 with the EstA (PDB ID code 2UZ0) and OLEI01171 (PDB ID code 3S8Y). The Est12, EstA, and OLEI01171 were shown in *green*, *magenta,* and *cyan,* respectively. **b** The caps domain in Est12 (residues 168–187 in *red*). **c** The caps domain in EstA (residues 145–178 in *blue*). **d** The caps domain in OLEI01171 (residues 171–216 in *magenta*)

the biochemistry and structure characteristics of this esterase have highly advantageous for its potential application as biocatalyst in commercial hydrolysis reactions which require alkaline, low temperature, and C_6 substrate.

Acknowledgments This work was supported by the National High Technology Research and Development Program of China (2007AA09Z443 and 2007AA021301), Knowledge Innovation Project of The Chinese Academy of Sciences (KSCX2-YW-G-022), the National Key Basic Research Program of China '973 Program' (2011CBA00803), and the Hundred Talents Program of the Chinese Academy of Sciences (Grant No. A1097). We cordially thank the staff of beamline BL17U1 at the Shanghai Synchrotron Radiation Facility, People's Republic of China for assistance in synchrotron X-ray data collection.

References

1. Adams PD, Afonine PV, Bunkoczi G, Chen VB, Davis IW, Echols N, Headd JJ, Hung LW, Kapral GJ, Grosse-Kunstleve RW, McCoy AJ, Moriarty NW, Oeffner R, Read RJ, Richardson DC, Richardson JS, Terwilliger TC, Zwart PH (2010) PHENIX: a comprehensive python-based system for macromolecular structure solution. Acta Crystallogr D 66:213–221
2. Amann RI, Ludwig W, Schleifer K-H (1995) Phylogenetic identification and in situ detection of individual microbial cells without cultivation. Microbiol Mol Biol R 59:143–169
3. Arpigny J, Jaeger K (1999) Bacterial lipolytic enzymes: classification and properties. Biochem J 343:177–183
4. Bendtsen JD, Nielsen H, von Heijne G, Brunak S (2004) Improved prediction of signal peptides: SignalP 3.0. J Mol Biol 340:783–795
5. Cavicchioli R, Siddiqui KS, Andrews D, Sowers KR (2002) Low-temperature extremophiles and their applications. Curr Opin Biotechnol 13:253–261
6. Chu X, He H, Guo C, Sun B (2008) Identification of two novel esterases from a marine metagenomic library derived from South China Sea. Appl Microbiol Biotechnol 80:615–625
7. Cottrell MT, Moore JA, Kirchman DL (1999) Chitinases from uncultured marine microorganisms. Appl Environ Microbiol 65:2553–2557
8. de Pascale D, Cusano AM, Autore F, Parrilli E, di Prisco G, Marino G, Tutino ML (2008) The cold-active Lip1 lipase from the Antarctic bacterium *Pseudoalteromonas haloplanktis* TAC125 is a member of a new bacterial lipolytic enzyme family. Extremophiles 12:311–323
9. De Santi C, Tedesco P, Ambrosino L, Altermark B, Willassen NP, de Pascale D (2014) A new alkaliphilic cold-active esterase from the psychrophilic marine bacterium *Rhodococcus* sp.: functional and structural studies and biotechnological potential. Appl Biochem Biotechnol 172:3054–3068
10. Delcher AL, Harmon D, Kasif S, White O, Salzberg SL (1999) Improved microbial gene identification with GLIMMER. Nucleic Acids Res 27:4636–4641
11. DeSantis G, Zhu Z, Greenberg WA, Wong K, Chaplin J, Hanson SR, Farwell B, Nicholson LW, Rand CL, Weiner DP (2002) An enzyme library approach to biocatalysis: development of nitrilases for enantioselective production of carboxylic acid derivatives. J Am Chem Soc 124:9024–9025
12. Emsley P, Lohkamp B, Scott WG, Cowtan K (2010) Features and development of coot. Acta Crystallogr D 66:486–501
13. Fang Z, Li J, Wang Q, Fang W, Peng H, Zhang X, Xiao Y (2014) A novel esterase from a marine metagenomic library exhibiting salt tolerance ability. J Microbiol Biotechnol 24:771–780
14. Feller G, Gerday C (1997) Psychrophilic enzymes: molecular basis of cold adaptation. Cell Mol Life Sci 53:830–841
15. Felsenstein J (1985) Confidence limits on phylogenies: an approach using the bootstrap. Evolution 39:783–791
16. Ferrer M, Martínez-Abarca F, Golyshin PN (2005) Mining genomes and 'metagenomes' for novel catalysts. Curr Opin Biotechnol 16:588–593
17. Fu C, Hu Y, Xie F, Guo H, Ashforth EJ, Polyak SW, Zhu B, Zhang L (2011) Molecular cloning and characterization of a new cold-active esterase from a deep-sea metagenomic library. Appl Microbiol Biotechnol 90:961–970
18. Fu J, Leiros HK, de Pascale D, Johnson KA, Blencke HM, Landfald B (2013) Functional and structural studies of a novel cold-adapted esterase from an Arctic intertidal metagenomic library. Appl Microbiol Biotechnol 97:3965–3978
19. Georlette D, Blaise V, Collins T, D'Amico S, Gratia E, Hoyoux A, Marx JC, Sonan G, Feller G, Gerday C (2004) Some like it cold: biocatalysis at low temperatures. FEMS Microbiol Rev 28:25–42
20. Gupta R, Beg Q, Lorenz P (2002) Bacterial alkaline proteases: molecular approaches and industrial applications. Appl Microbiol Biotechnol 59:15–32
21. Hårdeman F, Sjöling S (2007) Metagenomic approach for the isolation of a novel low-temperature-active lipase from uncultured bacteria of marine sediment. FEMS Microbiol Ecol 59:524–534
22. Hanson SR, Best MD, Wong CH (2004) Sulfatases: structure, mechanism, biological activity, inhibition, and synthetic utility. Angew Chem Int Ed 43:5736–5763

23. Henne A, Daniel R, Schmitz RA, Gottschalk G (1999) Construction of environmental DNA libraries in *Escherichia coli* and screening for the presence of genes conferring utilization of 4-hydroxybutyrate. Appl Environ Microbiol 65:3901–3907
24. Henne A, Schmitz RA, Bömeke M, Gottschalk G, Daniel R (2000) Screening of environmental DNA libraries for the presence of genes conferring lipolytic activity on *Escherichia coli*. Appl Environ Microbiol 66:3113–3116
25. Holm L, Rosenstrom P (2010) Dali server: conservation mapping in 3D. Nucleic Acids Res 38:W545–W549
26. Hu Y, Fu C, Huang Y, Yin Y, Cheng G, Lei F, Lu N, Li J, Ashforth EJ, Zhang L, Zhu B (2010) Novel lipolytic genes from the microbial metagenomic library of the South China Sea marine sediment. FEMS Microbiol Ecol 72:228–237
27. Hu Y, Fu C, Yin Y, Cheng G, Lei F, Yang X, Li J, Ashforth EJ, Zhang L, Zhu B (2010) Construction and preliminary analysis of a deep-sea sediment metagenomic fosmid library from Qiongdongnan Basin, South China Sea. Mar Biotechnol (NY) 12:719–727
28. Jaeger K-E, Eggert T (2002) Lipases for biotechnology. Curr Opin Biotechnol 13:390–397
29. Jeon JH, Kim JT, Lee HS, Kim SJ, Kang SG, Choi SH, Lee JH (2011) Novel lipolytic enzymes identified from metagenomic library of deep-sea sediment. Evid-Based Compl Alt 2011:271419
30. Joseph B, Ramteke PW, Thomas G (2008) Cold active microbial lipases: some hot issues and recent developments. Biotechnol Adv 26:457–470
31. Kennedy J, Marchesi JR, Dobson AD (2008) Marine metagenomics: strategies for the discovery of novel enzymes with biotechnological applications from marine environments. Microb Cell Fact 7:27
32. Kim E-Y, Oh K-H, Lee M-H, Kang C-H, Oh T-K, Yoon J-H (2009) Novel cold-adapted alkaline lipase from an intertidal flat metagenome and proposal for a new family of bacterial lipases. Appl Environ Microbiol 75:257–260
33. Kim MH, Kang BS, Kim S, Kim K-J, Lee CH, Oh B-C, Park S-C, Oh T-K (2008) The crystal structure of the estA protein, a virulence factor from *Streptococcus pneumoniae*. Proteins 70:578–583
34. López-López O, Cerdán M, Gonzalez-Siso M (2014) New extremophilic lipases and esterases from metagenomics. Curr Protein Pept Sci 15:445–455
35. Lee M-H, Lee C-H, Oh T-K, Song JK, Yoon J-H (2006) Isolation and characterization of a novel lipase from a metagenomic library of tidal flat sediments: evidence for a new family of bacterial lipases. Appl Environ Microbiol 72:7406–7409
36. Lee S-W, Won K, Lim HK, Kim J-C, Choi GJ, Cho KY (2004) Screening for novel lipolytic enzymes from uncultured soil microorganisms. Appl Microbiol Biotechnol 65:720–726
37. Lemak S, Tchigvintsev A, Petit P, Flick R, Singer AU, Brown G, Evdokimova E, Egorova O, Gonzalez CF, Chernikova TN, Yakimov MM, Kube M, Reinhardt R, Golyshin PN, Savchenko A, Yakunin AF (2012) Structure and activity of the cold-active and anion-activated carboxyl esterase OLEI01171 from the oil-degrading marine bacterium *Oleispira antarctica*. Biochem J 445:193–203
38. Levisson M, van der Oost J, Kengen SW (2007) Characterization and structural modeling of a new type of thermostable esterase from *Thermotoga maritima*. FEBS J 274:2832–2842
39. Li X, Qin L (2005) Metagenomics-based drug discovery and marine microbial diversity. Trends Biotechnol 23:539–543
40. Liu Y, Zhang Y, Cao X, Xue S (2013) Cloning, purification, crystallization and preliminary X-ray crystallographic analysis of MCAT from *Synechocystis* sp PCC 6803. Acta Crystallogr F 69:1256–1259
41. Lorenz P, Eck J (2005) Metagenomics and industrial applications. Nat Rev Microbiol 3:510–516
42. McCoy AJ, Grosse-Kunstleve RW, Adams PD, Winn MD, Storoni LC, Read RJ (2007) Phaser crystallographic software. J Appl Crystallogr 40:658–674
43. Nam KH, Kim MY, Kim SJ, Priyadarshi A, Lee WH, Hwang KY (2009) Structural and functional analysis of a novel EstE5 belonging to the subfamily of hormone-sensitive lipase. Biochem Biophys Res Commun 379:553–556
44. Otwinowski Z, Minor W (1997) Processing of X-ray diffraction data collected in oscillation mode. In: Charles W. Carter, Jr. (Ed.), Methods in enzymology, edn. Academic Press, Waltham pp 307–326
45. Park H-J, Jeon JH, Kang SG, Lee J-H, Lee S-A, Kim H-K (2007) Functional expression and refolding of new alkaline esterase, EM2L8 from deep-sea sediment metagenome. Protein Expres Purif 52:340–347
46. Peng Q, Zhang X, Shang M, Wang X, Wang G, Li B, Guan G, Li Y, Wang Y (2011) A novel esterase gene cloned from a metagenomic library from neritic sediments of the South China Sea. Microb Cell Fact 10:95
47. Ranjan R, Grover A, Kapardar RK, Sharma R (2005) Isolation of novel lipolytic genes from uncultured bacteria of pond water. Biochem Biophys Res Commun 335:57–65
48. Rashid N, Shimada Y, Ezaki S, Atomi H, Imanaka T (2001) Low-temperature lipase from *Psychrotrophic Pseudomonas* sp. strain KB700A. Appl Environ Microbiol 67:4064–4069
49. Santarossa G, Lafranconi PG, Alquati C, DeGioia L, Alberghina L, Fantucci P, Lotti M (2005) Mutations in the "lid" region affect chain length specificity and thermostability of a *Pseudomonas fragi* lipase. FEBS Lett 579:2383–2386
50. Siddiqui KS, Cavicchioli R (2006) Cold-adapted enzymes. Annu Rev Biochem 75:403–433
51. Simons J-WF, van Kampen MD, Ubarretxena-Belandia I, Cox RC, Alves dos Santos CM, Egmond MR, Verheij HM (1999) Identification of a calcium binding site in *Staphylococcus hyicus* lipase: generation of calcium-independent variants. Biochemistry 38:2–10
52. Takami H, Kobata K, Nagahama T, Kobayashi H, Inoue A, Horikoshi K (1999) Biodiversity in deep-sea sites located near the south part of Japan. Extremophiles 3:97–102
53. Tamura K, Dudley J, Nei M, Kumar S (2007) MEGA4: molecular evolutionary genetics analysis (MEGA) software version 4.0. Mol Biol Evol 24:1596–1599
54. Thompson JD, Higgins DG, Gibson TJ (1994) CLUSTAL W: improving the sensitivity of progressive multiple sequence alignment through sequence weighting, position-specific gap penalties and weight matrix choice. Nucleic Acids Res 22:4673–4680
55. Verger R (1997) 'Interfacial activation'of lipases: facts and artifacts. Trends Biotechnol 15:32–38
56. Voget S, Steele H, Streit W (2006) Characterization of a metagenome-derived halotolerant cellulase. J Biotechnol 126:26–36
57. Winn MD, Ballard CC, Cowtan KD, Dodson EJ, Emsley P, Evans PR, Keegan RM, Krissinel EB, Leslie AGW, McCoy A, McNicholas SJ, Murshudov GN, Pannu NS, Potterton EA, Powell HR, Read RJ, Vagin A, Wilson KS (2011) Overview of the CCP4 suite and current developments. Acta Crystallogr D 67:235–242
58. Yun J, Kang S, Park S, Yoon H, Kim M-J, Heu S, Ryu S (2004) Characterization of a novel amylolytic enzyme encoded by a gene from a soil-derived metagenomic library. Appl Environ Microbiol 70:7229–7235
59. Zhang S, Wu G, Liu Z, Shao Z, Liu Z (2014) Characterization of EstB, a novel cold-active and organic solvent-tolerant esterase from marine microorganism *Alcanivorax dieselolei* B-5 (T). Extremophiles 18:251–259